

148

BBC

ENGINEERING DIVISION

MONOGRAPH

NUMBER 54 : AUGUST 1964

**An Analysis of Film Granularity
in Television Reproduction**

by

K. HACKING, B.Sc.

(Research Department, BBC Engineering Division)

BRITISH BROADCASTING CORPORATION

PRICE FIVE SHILLINGS



BBC ENGINEERING MONOGRAPH

No. 54

AN ANALYSIS OF FILM GRANULARITY
IN TELEVISION REPRODUCTION

by

K. Hacking, B.Sc.

(Research Department, BBC Engineering Division)

AUGUST 1964

BRITISH BROADCASTING CORPORATION

FOREWORD

THIS is one of a series of Engineering Monographs published by the British Broadcasting Corporation. About six are produced every year, each dealing with a technical subject within the field of television and sound broadcasting. Each Monograph describes work that has been done by the Engineering Division of the BBC and includes, where appropriate, a survey of earlier work on the same subject. From time to time the series may include selected reprints of articles by BBC authors that have appeared in technical journals. Papers dealing with general engineering developments in broadcasting may also be included occasionally.

This series should be of interest and value to engineers engaged in the fields of broadcasting and of telecommunications generally.

Individual copies cost 5s. post free, while the annual subscription is £1 post free. Orders can be placed with newsagents and booksellers, or BBC PUBLICATIONS, 35 MARYLEBONE HIGH STREET, LONDON, W.1.

CONTENTS

<i>Section</i>	<i>Title</i>	<i>Page</i>
	PREVIOUS ISSUES IN THIS SERIES	4
	SUMMARY	5
1.	INTRODUCTION	5
2.	BASIC PARAMETERS	5
2.1	The Scanning Aperture	5
2.1.1	Scanning Beam Size and Initial Signal-to-noise Ratio	6
2.2	Spectrum Filtering and Equalization	8
2.2.1	Equivalent Apertures	8
2.2.2	Ideal Equivalent Apertures	10
2.2.3	Effect on Granularity Transfer	10
3.	ELECTRICAL NOISE-POWER SPECTRUM	12
4.	COMPARISON OF NEGATIVE-TYPE EMULSIONS	12
5.	FILM PROCESSING	12
5.1	Variation of Signal-to-noise Ratio with Density	12
5.2	Effect of Development Gamma	14
6.	SIGNAL PROCESSING	15
7.	DISPLAYED GRANULARITY	16
7.1	Granularity Distribution Curves	16
7.1.1	Negative-to-positive Process (Method II, Section 5.1)	16
7.1.2	Direct-positive Process (Method I, Section 5.1)	16
7.1.3	Direct-negative Process (Method IV, Section 5.1)	17
7.1.4	Reversal Process (Method III, Section 5.1)	17
7.1.5	Effect of Over-exposure	17
7.2	Granularity Spectrum	18
8.	SUBJECTIVE ASSESSMENTS	18
8.1	Visual Thresholds	18
8.2	Visual Sensitivity	19
8.3	Displayed Granularity	20
8.4	Numerical Examples	20
9.	CONCLUSIONS	20
10.	ACKNOWLEDGMENTS	21
11.	REFERENCES	21
	APPENDIX	22

PREVIOUS ISSUES IN THIS SERIES

No.	Title	Date
1.	<i>The Suppressed Frame System of Telerecording</i>	JUNE 1955
2.	<i>Absolute Measurements in Magnetic Recording</i>	SEPTEMBER 1955
3.	<i>The Visibility of Noise in Television</i>	OCTOBER 1955
4.	<i>The Design of a Ribbon Type Pressure-gradient Microphone for Broadcast Transmission</i>	DECEMBER 1955
5.	<i>Reproducing Equipment for Fine-groove Records</i>	FEBRUARY 1956
6.	<i>A V.H.F./U.H.F. Field-strength Recording Receiver using Post-detector Selectivity</i>	APRIL 1956
7.	<i>The Design of a High Quality Commentator's Microphone Insensitive to Ambient Noise</i>	JUNE 1956
8.	<i>An Automatic Integrator for Determining the Mean Spherical Response of Loudspeakers and Microphones</i>	AUGUST 1956
9.	<i>The Application of Phase-coherent Detection and Correlation Methods to Room Acoustics</i>	NOVEMBER 1956
10.	<i>An Automatic System for Synchronizing Sound on Quarter-inch Magnetic Tape with Action on 35-mm Cinematograph Film</i>	JANUARY 1957
11.	<i>Engineering Training in the BBC</i>	MARCH 1957
12.	<i>An Improved 'Roving Eye'</i>	APRIL 1957
13.	<i>The BBC Riverside Television Studios: The Architectural Aspects</i>	JULY 1957
14.	<i>The BBC Riverside Television Studios: Some Aspects of Technical Planning and Equipment</i>	OCTOBER 1957
15.	<i>New Equipment and Methods for the Evaluation of the Performance of Lenses for Television</i>	DECEMBER 1957
16.	<i>Analysis and Measurement of Programme Levels</i>	MARCH 1958
17.	<i>The Design of a Linear Phase-shift Low-pass Filter</i>	APRIL 1958
18.	<i>The BBC Colour Television Tests: An Appraisal of Results</i>	MAY 1958
19.	<i>A U.H.F. Television Link for Outside Broadcasts</i>	JUNE 1958
20.	<i>The BBC's Mark II Mobile Studio and Control Room for the Sound Broadcasting Service</i>	AUGUST 1958
21.	<i>Two New BBC Transparencies for Testing Television Camera Channels (Out of Print)</i>	NOVEMBER 1958
22.	<i>The Engineering Facilities of the BBC Monitoring Service</i>	JANUARY 1959
23.	<i>The Crystal Palace Band I Television Transmitting Aerial</i>	FEBRUARY 1959
24.	<i>The Measurement of Random Noise in the presence of a Television Signal</i>	MARCH 1959
25.	<i>A Quality-checking Receiver for V.H.F. F.M. Sound Broadcasting</i>	JUNE 1959
26.	<i>Transistor Amplifiers for Sound Broadcasting</i>	AUGUST 1959
27.	<i>The Equipment of the BBC Television Film Studios at Ealing</i>	JANUARY 1960
28.	<i>Programme Switching, Control, and Monitoring in Sound Broadcasting</i>	FEBRUARY 1960
29.	<i>A Summary of the Present Position of Stereophonic Broadcasting</i>	APRIL 1960
30.	<i>Film Processing and After-processing Treatment of 16-mm Films</i>	MAY 1960
31.	<i>The Power Gain of Multi-tiered V.H.F. Transmitting Aerials</i>	JULY 1960
32.	<i>A New Survey of the BBC Experimental Colour Transmissions</i>	OCTOBER 1960
33.	<i>Sensitometric Control in Film Making</i>	DECEMBER 1960
34.	<i>A Mobile Laboratory for UHF and VHF Television Surveys</i>	FEBRUARY 1961
35.	<i>Tables of Horizontal Radiation Patterns of Dipoles Mounted on Cylinders</i>	FEBRUARY 1961
36.	<i>Some Aspects of Optical Lens Performance</i>	APRIL 1961
37.	<i>An Instrument for Measuring Television Signal-to-noise Ratio</i>	JUNE 1961
38.	<i>Operational Research on Microphone and Studio Techniques in Stereophony</i>	SEPTEMBER 1961
39.	<i>Twenty-five Years of BBC Television</i>	OCTOBER 1961
40.	<i>The Broadcasting of Music in Television</i>	FEBRUARY 1962
41.	<i>The Design of a Group of Plug-in Television Studio Amplifiers</i>	APRIL 1962
42.	<i>Apparatus for Television and Sound Relay Stations</i>	JULY 1962
43.	<i>Propagational Factors in Short-wave Broadcasting</i>	AUGUST 1962
44.	<i>A Band V Signal-frequency and a Correlation Detector for a VHF/UHF Field-strength Recording Receiver</i>	OCTOBER 1962
45.	<i>Vertical Resolution and Line Broadening</i>	DECEMBER 1962
46.	<i>The Application of Transistors to Sound Broadcasting</i>	FEBRUARY 1963
47.	<i>Vertical Aperture Correction using Continuously Variable Ultrasonic Delay Lines</i>	MAY 1963
48.	<i>The Development of BBC Internal Telecommunications</i>	MAY 1963
49.	<i>Apparatus for Measurement of Non-linear Distortion as a Continuous Function of Frequency</i>	JULY 1963
50.	<i>New Methods of Lens Testing and Measurement</i>	SEPTEMBER 1963
51.	<i>Radiophonics in the BBC</i>	NOVEMBER 1963
52.	<i>Stereophony: the effect of cross-talk between left and right channels</i>	MARCH 1964
53.	<i>Aerial distribution systems for receiving stations in the l.f., m.f., and h.f. bands</i>	JUNE 1964

AN ANALYSIS OF FILM GRANULARITY IN TELEVISION REPRODUCTION

SUMMARY

The transfer of emulsion granularity in a television system when film is the picture source is considered in some detail using the Wiener spectrum of the film-grain to describe its near-random statistical properties. The modifying effects of some basic parameters associated with television film-scanning and the subsequent processing of the generated video signal are discussed, and illustrated by numerical examples based on the measured Wiener spectra of several commonly-used black-and-white cine-film emulsions.

The differences in the character and magnitude of the granularity obtained in the final display, due to the several methods and processes employed in the various television applications of film are examined. Displayed granularity curves are deduced for each of four processes, by selecting appropriate emulsions and by assuming specific processing conditions considered to be representative of operational practice.

After discussing briefly several important factors associated with the visibility of the displayed granularity an attempt is made to establish, from existing experimental evidence, realistic thresholds of perceptibility in terms of the standard deviation of luminance in the display. Finally, the probable subjective rating, on a six-point scale, of the displayed granularity is deduced for the specific examples representing the four main processes mentioned earlier.

1. Introduction

In a television system, using film as the picture source, an important contribution to the total random noise accompanying the signal applied to the display tube may be that due to the granularity of the film. Indeed, when the noise levels due to the various electrical sources in the transmission path are kept low, film-grain can be the limiting factor to the noise-free quality of the reproduction. Modern developments in the components and circuits associated with electro-optical devices are often aimed at improving the signal-to-noise ratio of the system. Likewise, the development of photographic emulsions is often directed towards greater sensitivity with finer grain. However, not all transmissions are free from visible noise, and there is often room for improving the overall signal-to-noise ratio of the system in spite of the highly-developed state of the art.

Unfortunately, on many occasions when the picture source is cine-film the quality of the reproduction is marred by macro-blemishes of, or in, the film, due to dirt, scratches, hairs, etc., occurring during its processing or projection. Perhaps it is too unrealistic to say that these are avoidable defects but they are, nevertheless, artifacts of the process and their integrated visual effect may certainly be regarded as objectionable noise—although not the kind that invites a quantitative analysis. However, when all other defects are removed, the inherent granularity of the developed emulsion sets an upper limit to the signal-to-noise ratio of the reproduction.

A comprehensive analytical treatment of television random noise has been given by Schade,¹ and some of the same ground is covered here. The present analysis is concerned with the transfer of emulsion granularity in television from the standpoint of the two-dimensional spectral analysis of the developed grain structure and its subsequent modification by the transmission system. The quantitative examples are all based on the results of granularity investigations by the author of several commercial cine-

film emulsions.* Finally, a brief attempt is made to assess, quantitatively, over a range of luminance levels, the visibility of the luminance noise in the reproduction.

Before dealing with the effects of some basic parameters on the transferred granularity, it should be pointed out that the analysis refers always to the granularity in areas of coarse picture detail (i.e. background fluctuation noise in those regions of the picture where the mean luminance or density level is substantially uniform). Thus, the effects of noise on the reproduction of vertical edges, and possible inter-modulation effects arising from the signal processing, are not considered.

2. Basic Parameters

2.1 *The Scanning Aperture*

The picture signal is generated by scanning either the film itself or an optically projected image of the film with a fine beam (optical or electronic). In either method the actual scanning beam will be of finite cross-section which, together with its lateral intensity profile, will be determined by the design and operating parameters of the electro/optical components of the particular film scanner. Within certain practical limits, therefore, the actual size of the scanning beam is under the control of the design engineer.

It is well known that the effect of scanning with a beam of finite cross-section (aperture effect) is to weight or modify the Fourier spectrum of the recorded or stored information, often simply by attenuating the amplitude of the high-frequency components. Subsequent filtering and equalizing operations on the output signal of the scanner can be regarded as counteracting and/or further modifying the effect of the actual scanning beam. Thus, an identical

* Only black-and-white emulsions have been measured, although the general analysis given in this report is applicable to colour films. The measurements were made with an optical picture correlator, using photomicrographs of the grain structures obtained when the emulsions are uniformly exposed to light and developed in the normal manner.

signal would be obtained if the film was scanned initially with a hypothetical scanning beam (termed the 'equivalent scanning aperture'), having the same spectrum-weighting effect as that of the actual scanning beam combined with that of the subsequent signal processing. If the system nonlinearities can be neglected (as is possible for small signal fluctuations and noise) the idea can be extended to the complete television system, the latter being then described by its equivalent scanning aperture. A full treatment of aperture theory applied to the television process has been given by Schade.²

Normally, the size of the actual scanning spot in a film scanner will be commensurate with that of a television picture element (referred to the scanned film-frame), and such as to maintain reasonable vertical resolution since, as yet, correction for the aperture effect in the vertical direction* is not usually employed.

Let us suppose that we are dealing with a flying-spot film scanner, and that the initial part of the signal processing, following the photomultiplier output, is as shown in Fig. 1, which is a block schematic diagram indicating the main signal-processing operations in a conventional scanner.†

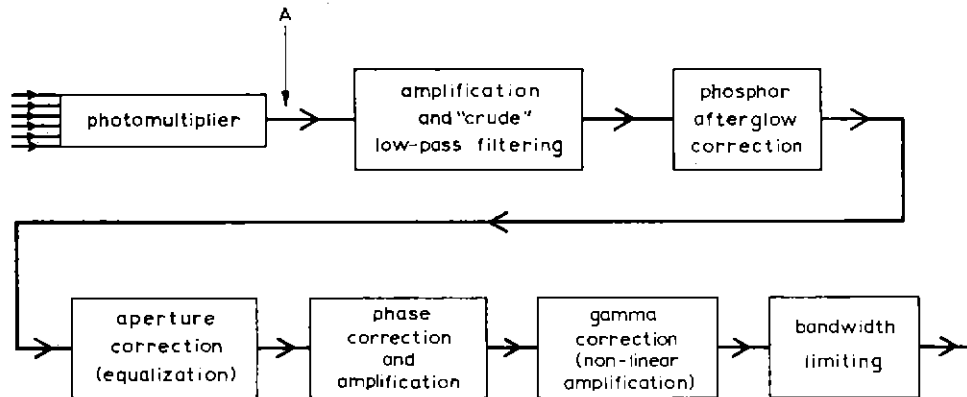


Fig. 1 — Signal processing operations in a conventional flying-spot scanner

It is instructive to consider first, the statistical magnitude and power-spectral density of the electrical noise (due to film granularity) directly at the photomultiplier output and then, later, the modifying effects of subsequent signal-processing operations. It is assumed that the photomultiplier and its associated electrical amplifier are perfect, or have been perfectly corrected, and do not introduce additional signal distortions.

2.1.1 Scanning Beam Size and Initial Signal-to-noise Ratio

It is easy to appreciate that the larger the cross-section of the scanning beam the smaller will be the magnitude of the average modulation introduced by the granular structure of the film. It may be shown that the signal-to-

r.m.s. noise ratio at the scanner output, when the beam is traversing an area of the film of given mean optical density, is inversely proportional to the square root of M , where

$$M = \iint_{(\infty)} N(f_x, f_y) |V(f_x, f_y)|^2 df_x df_y \quad (1)$$

Here $N(f_x, f_y)$ is the grain Wiener spectrum* of the film being scanned and $V(f_x, f_y)$ is the frequency response function of the scanning aperture. The variables f_x and f_y are spatial frequency co-ordinates corresponding respectively to the directions of a pair of rectangular co-ordinate axes (x, y) , supposed to exist in the surface of the film. Now, in a flying-spot scanner, the lateral intensity distribution of light flux in the scanning beam is that of the flying spot on the cathode-ray tube (c.r.t.) modified by the imaging optical lens: and, in a practical scanner, the intensity distribution may depend on the lateral position of the beam in the scanned field. For example, the c.r.t. flying-spot may defocus slightly towards the edges of the field and/or the lens aberrations may vary considerably with field position. Thus in equation (1) $|V(f_x, f_y)|$, which is simply the modulus

of the two-dimensional Fourier transform of the beam intensity profile, is likely to be a (slowly varying) function of the field position. The grain Wiener spectrum $N(f_x, f_y)$ is unlikely to be dependent on the field position, although some dependence could occur in, say, a print where the granularity has been modified by the printing optics.

The integrand of equation (1) may be termed the modified or aperture-weighted Wiener spectrum, $N'(f_x, f_y)$. It may be helpful to regard the actual grain Wiener spectrum as replaced by $N'(f_x, f_y)$ and the scanning beam to be of vanishingly small cross-section—the modulation of the output signal is identical with that arising from the former concept.

It will be noted that the integrand of equation (1) is a two-dimensional function and can, therefore, be repre-

* This is the two-dimensional optical equivalent of the power-spectrum of electrical random-noise. See reference 3 for a discussion of the Wiener spectrum concept applied to granularity.

• It is assumed that the scanning direction is horizontal.

† Not necessarily performed in the order shown.

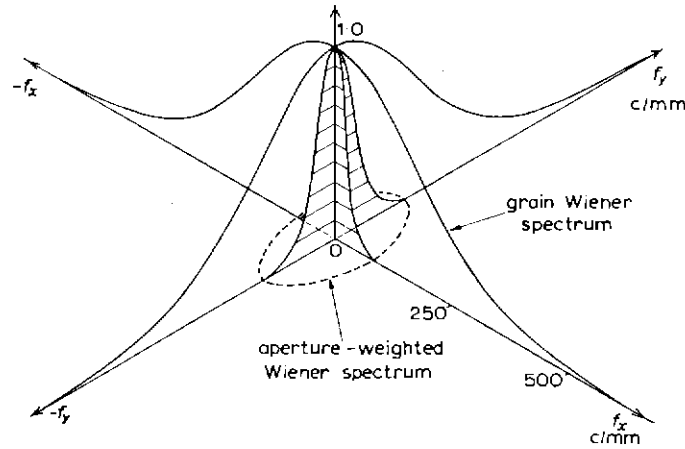


Fig. 2 — Typical grain Wiener spectra

sented graphically by a solid figure; also, that M is equal to the volume of the solid figure, i.e. to the volume under the modified Wiener spectrum, $N'(f_x, f_y)$. The weighting process is illustrated in Fig. 2, where two right sections of a typical normalized grain Wiener spectrum and (shaded) the effect of a finite-size scanning aperture are shown. In constructing the figure the scanning aperture was arbitrarily chosen to be somewhat elongated in the x co-ordinate direction,* i.e. the two-dimensional representation of the scanning beam intensity-profile does not have circular symmetry. In point of fact, the equivalent aperture is usually asymmetrical due to the phosphor afterglow of the flying-spot tube, even if the actual scanning beam itself has circular symmetry when arrested. Clearly, deliberate line-broadening techniques⁴ such as spot-wobble and astigmatic imagery (electronic and optical) give rise to asymmetric scanning apertures.

The statistical properties of the developed grain structure of commercial emulsions appear to be substantially isotropic, so that their Wiener spectra have circular symmetry and can be specified by their generating curves (radial profiles); as a specific example, the grain Wiener spectrum of Kodak 8374, a 16-mm television film recording emulsion, deduced from autocorrelation measurements on a uniformly exposed sample, is shown by the full line in Fig. 3(a). The overall development gamma and mean optical density of the measured sample is indicated on the figure. The dashed-line is the weighted spectrum assuming convolution with a symmetrical beam having a Gaussian intensity profile:† the weighting function $|V(f)|^2$ is given by

$$|V(f)|^2 = e^{-1.4(f/f_c)^2}$$

where f_c is the spatial frequency at which the aperture frequency response characteristic (i.e. $|V(f)|$) has fallen by

* In what follows the x co-ordinate direction is taken to be the direction of the line scan.

† Actual measurements on a flying-spot tube having a P16 phosphor, carried out by colleagues E. R. Rout and W. N. Sproson, showed the beam intensity profile to be very closely Gaussian (afterglow neglected).

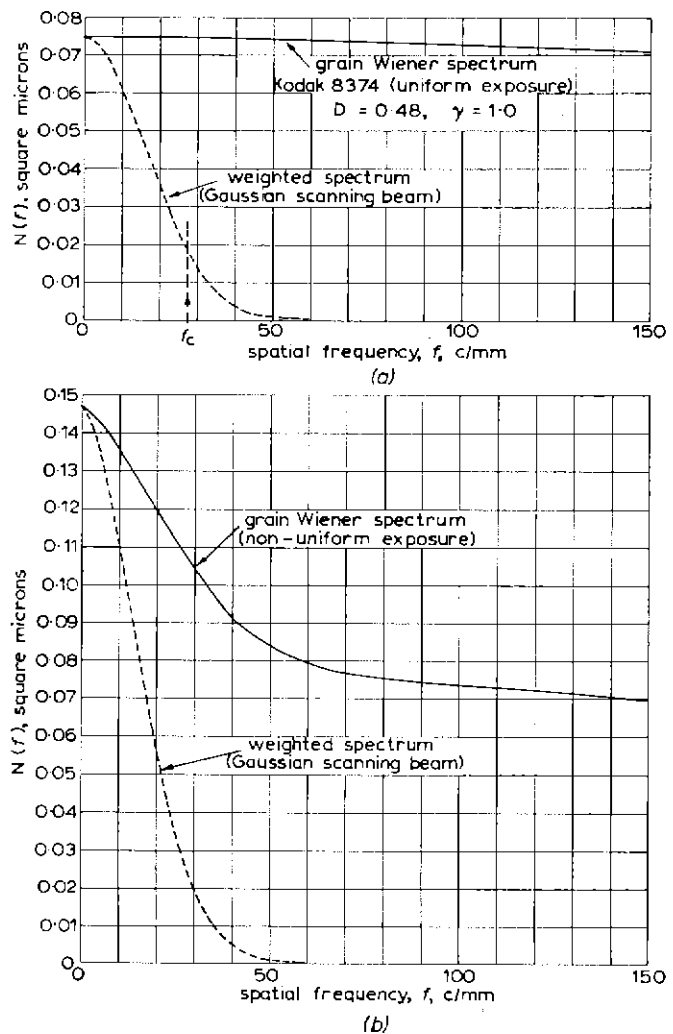


Fig. 3 — Grain Wiener spectra (radial sections) of Kodak 8374

- (a) Uniform exposure
- (b) Non-uniform exposure 8374 printed on 8374

6 dB. If, as assumed in Fig. 3, $f_c=28$ cycles/mm, which corresponds to the cut-off frequency of 5 Mc/s used in many CCIR 625/50 television standards applied to 16-mm gauge film, the scanning beam diameter will be approximately 16.7 microns, measured at the $e^{-\pi/4}$ level of intensity.

Fig. 3(b) is similar to 3(a), but refers to the situation where the grain Wiener spectrum is not uniform, as in a positive print. The Wiener spectrum shown in Fig. 3(b) is derived from the measured Wiener spectrum by supposing that the same type of emulsion, namely Kodak 8374, is used for both negative and positive: the measured sample is assumed to be contact printed such that the resulting positive print has the same optical density as the negative when developed to the same gamma.

this simple and well-known relationship* does not strictly hold for non-uniform spectra.

A second abscissae scale is included in Fig. 4 which shows the cut-off frequencies (i.e. the 6 dB points as defined earlier) in cycles/mm corresponding to the beam-diameters of the first scale. If the cut-off frequency is regarded as the intrinsic resolving power of the scanner we note that the figure now clearly emphasises the oft-encountered possibility of trading resolving power for signal-to-noise ratio.

2.2 Spectrum Filtering and Equalization

2.2.1 Equivalent Apertures

The effects of subsequent signal processing, band-pass filtering, and equalization operations on the r.m.s. magni-

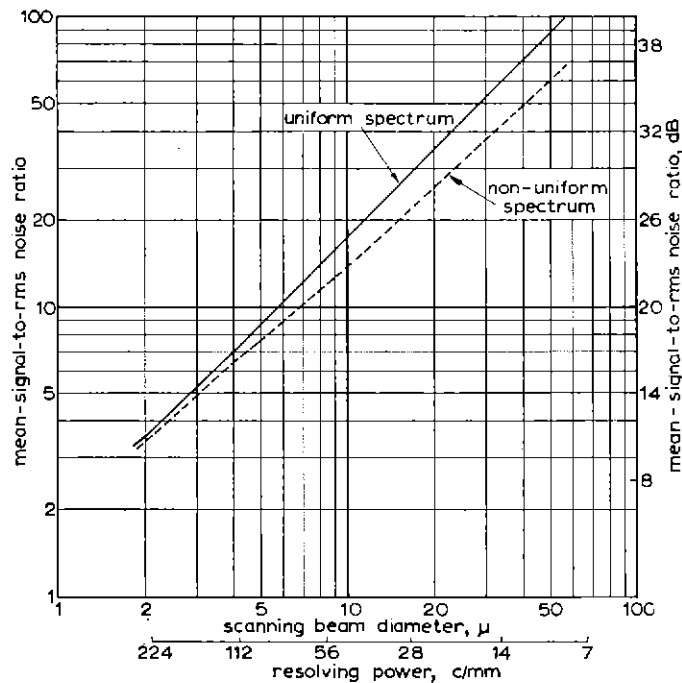


Fig. 4 — Relationship between scanning beam diameter and output signal-to-noise ratio

If these samples of the Kodak 8374 emulsion are placed in a flying-spot scanner having a symmetrical (Gaussian) scanning beam, the large-area signal-to-noise ratios, referred to henceforth as mean-signal-to-r.m.s. noise ratios, at the photomultiplier output (point A in Fig. 1) will not be greater than is shown in Fig. 4, where the mean-signal-to-r.m.s. noise ratio is plotted against scanning beam diameter in microns, using logarithmic co-ordinate scales. The full-line refers to the sample with the uniform spectrum and the dashed-line to that of the printed sample with the non-uniform spectrum.

Fig. 4 shows that when the granularity spectrum is substantially uniform, over the spatial frequency range of interest, the output signal-to-r.m.s. noise ratio varies linearly with the spot diameter. It will be seen, also, that

tude and spectrum of the signal and its accompanying fluctuation noise are well known. Equalization to correct for the trailing frequency response characteristic of the effective scanning aperture is usually restricted to the line direction, but recent delay-line developments⁵ are providing a useful electrical means of achieving aperture-correction in the vertical direction.

It is interesting to refer back these filtering processes, which occur in the (one-dimensional) electrical phase of the transmission, by considering their equivalent weighting effects on the original (two-dimensional) Wiener spectrum of the grain. Fig. 5 illustrates the general inter-

* This relationship is the basis of the Selwyn granularity measure. See, for instance, reference 7.

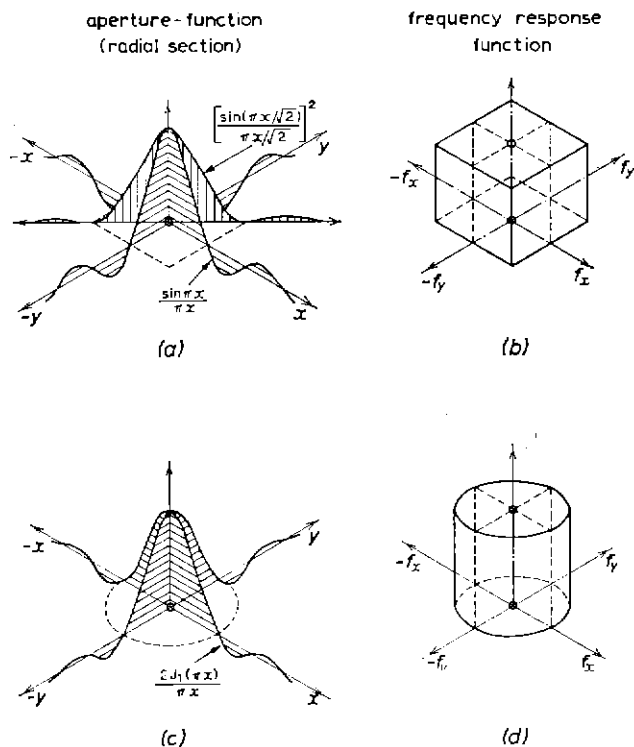


Fig. 6 — Ideal scanning apertures and their Fourier transforms

the positive and negative spatial frequencies corresponding respectively to the cut-off frequencies of the filter. The filter shown at (b) is similar to that at (a) but provides equalization or 'top lift' in addition to bandwidth restriction. The equivalent aperture of this filter has a two-dimensional Wiener spectral-weighting function $\Pi(b)$ which resembles a channel of terminated section parallel to the direction of scan and of unbounded 'constant' section orthogonally. At (c) the same electrical filter (b) is assumed to be effectively applied in both the x and y directions: this corresponds to the situation where both horizontal and vertical* low-pass filtering (with equalization) is achieved by electrical means. The equivalent two-dimensional filter is now bounded in both directions and gives rise to the 'molar' shaped noise-power weighting function shown at $\Pi(c)$.

2.2.2 Ideal Equivalent Apertures

An equivalent scanning aperture which allows the maximum amount of real picture information to be transferred for a given video channel bandwidth, and equal horizontal and vertical resolution is shown in Fig. 6(a) and has the frequency response function shown in Fig.

* Strictly, in a line-scanning process with finite line-density, L say, it is not possible to achieve, by subsequent electrical devices only, ideal low-pass filtering such that all vertical spectrum components of the picture of spatial frequency greater than $L/2$ are completely eliminated. However, in association with a scanning spot having a suitably broadened line-intensity profile a good approximation to the ideal equivalent aperture can be obtained.

6(b). A practical approach to this situation would be, for instance, an extremely fine scanning beam to which is applied modulated spot-wobble¹ in the vertical direction followed by well-corrected electrical low-pass filtering in the video channel. It is worth noting that such an equivalent aperture does not have circular symmetry, and it may be seen from Fig. 6(b) that the resolving power is greatest in the diagonal direction (in fact, $\sqrt{2}$ times the horizontal or vertical resolution).

A symmetrical form of equivalent aperture is shown in Fig. 6(c), and has the frequency response function shown in Fig. 6(d). The system is seen to have equal resolving power in all directions because of the circular symmetry of the equivalent aperture. This type of aperture lends itself to an optical method of generation, but it is difficult to realize in practice because a coherent light source is required. One possible method* may be to use the coherent beam generated by a suitable optical maser to illuminate the film which is then imaged by a lens, having a circular stop of the required diameter, on to a high-resolution camera tube.

2.2.3 Effect on Granularity Transfer

The quantitative effects of filtering and equalization, on the transfer of granularity, and the comparison of the above ideal apertures with some other forms of aperture, are illustrated in Fig. 7 by some numerical examples of the mean-signal-to-r.m.s. noise ratio at several stages of signal processing. As a basis for comparison it is assumed that an area of uniform optical density (approximately 0.5 above base) of Kodak Plus-X, a negative-type panchromatic emulsion, is being scanned.[†] It is supposed, further, that low-pass filtering limits the spatial frequency range to 28 cycles/mm; this corresponds to a 5 Mc/s video bandwidth, as used in many 625/50 European standards, in conjunction with 16-mm gauge cine-film.

In Fig. 7, the first group of scanning apertures ((a) to (d)) involve scanning beams having Gaussian intensity profiles and are typical of those which may be readily achieved in actual flying-spot scanners (neglecting phosphor afterglow effects). The remaining group of apertures ((e) to (h)) are included mainly for theoretical interest.

Aperture (c) is the symmetrical Gaussian scanning beam I, shown at (a) to which vertical, sinusoidal, spot-wobble has been applied. (First zero of the vertical frequency response function is chosen to occur at approximately 80 cycles/mm.) Aperture (d) is the larger-diameter Gaussian beam II, shown at (b), with modulated spot-wobble⁴ applied to the scanner such that the ideal, $(\sin \pi u)/\pi u$, vertical line-profile is simulated as far as the first negative lobe, i.e. up to $u = 2$.

A general conclusion which may be noted from the data in Fig. 7 is that, if vertical spot-wobble is not available, it is better to avoid using too fine a scanning beam in order that

* Not suitable for a colour scanner.

† The grain Wiener spectrum of this emulsion has been measured at this particular density, and the low-frequency portion of the spectrum is shown in Fig. 8.

SCANNING APERTURE		APERTURE FREQUENCY RESPONSE FUNCTION ($f =$ spatial frequency, cycles/mm)		MEAN-SIGNAL-TO-RMS-NOISE RATIO*		
				AT PHOTOMULTIPLIER OUTPUT	AFTER BANDWIDTH LIMITING	AFTER LIMITING AND HORIZONTAL APERTURE CORRECTION
	TYPE	HORIZONTAL	VERTICAL	dB	dB	dB
(a)	GAUSSIAN I			21.6	23.5	22.8
(b)	GAUSSIAN II			27.7	28	25.8
(c)	GAUSSIAN I with sinusoidal spot-wobble			23.3	25.2	24.5
(d)	GAUSSIAN II with modulated spot-wobble**			25	25.3	23.1
(e)	DIFFRACTION LIMITED POINT (numerical aperture 0.65)			1.6	13	none required
(f)	'PIN-HOLE' (26 microns diameter)			25.6	26.6	25.7
(g)	IDEAL APERTURE (asymmetrical)			24	self-limiting	none required
(h)	IDEAL APERTURE (symmetrical)			25	self-limiting	none required

Fig. 7 — Variation of signal-to-noise ratio with form of scanning aperture

* Kodak Plus-X at density of 0.48 (uniform exposure) assumed to be scanned

** Simulation of ideal $(\sin \pi u)/\pi u$ profile up to $u = 2$ only

a reasonable amount of spectrum filtering in the vertical direction is achieved by the beam itself.*

3. Electrical Noise-Power Spectrum

A general theory of granularity transfer by sequential line-scanning in a linear television system is briefly developed in an Appendix to this report. However, from equation (1) in Section 2.1.1 we see that for a given mean-signal the electrical noise-power at the photomultiplier output is proportional to M , where

$$M = \iint_{(-\infty)} N'(f_x, f_y) df_x df_y \quad (2)$$

remembering that

$$N'(f_x, f_y) \equiv N(f_x, f_y) |V(f_x, f_y)|^2$$

Rewriting equation (2) in the form

$$M = \int_{-\infty}^{+\infty} P(f_x) df_x \quad (3)$$

where

$$P(f_x) \equiv \int_{-\infty}^{+\infty} N'(f_x, f_y) df_y$$

we note that, from an energy point of view, the integrand $P(f_x)$ in equation (3) can be regarded as the power spectrum of the electrical noise since its infinite integral gives the total noise power M . As defined above, $P(f_x)$ is a rigorous mathematical description of the noise-power spectrum only when the scan is a single straight line of infinite length in the x direction. As shown in the Appendix, the actual power spectral density of the noise resulting from a picture scan by a finite number of parallel lines has a structure which depends on the scanning parameters and, in particular, on the scanning line-density (lines/unit height). If the line-density is high the noise-power spectral density function may have pronounced peaks at harmonics of the line scan frequency (see Fig. 19(b) in the Appendix), and it may be argued that the form of the function is then effectively described by the locus of the peaks. It is shown in the Appendix that this locus is given approximately by $N'(f_x, 0)$. In most actual television systems, either $P(f_x)$ or $N'(f_x, 0)$ can be regarded as broadly describing the form of the electrical noise-power spectrum since the difference between the two functions lies mainly in the vertical scale factor, especially in systems with scanning beam profiles of approximately Gaussian form.

In general, if the grain Wiener spectrum of the film is uniform, over the spectral range of interest, the electrical noise-power spectrum (as defined by equation (3)) at the final output of a fully-corrected video channel will also be uniform.

4. Comparison of Negative-type Emulsions

The low-frequency portions of the grain Wiener spectra of

* It may be shown that not only is the total noise-power at the scanner output increased by using a very fine scanning beam but also, and perhaps of greater importance subjectively, the peak (low-frequency) region of the displayed Wiener spectrum (see Appendix) is increased due to the transfer of the granularity by a finite number of scanning lines.

four negative-type, 35-mm gauge, cine-film emulsions are shown in Fig. 8, where the ordinate units are square microns and the abscissae are spatial frequencies in cycles/mm. The spectra refer to uniformly exposed samples of these emulsions developed (standard negative developer) to approximately the same gamma.* The mean optical density of each sample was approximately 0.48 above base density, measured on an E.E.L. densitometer.

The particular emulsions are listed in Table 1, together with their respective film-speed ratings, arithmetical and logarithmic, for tungsten illumination. Also given in the table is the mean level of the Wiener spectrum, over the range 0 to 20 cycles/mm, for each emulsion.

The relationship between the Wiener spectrum and the film-speed, for these particular emulsions, is shown in Fig. 9 which is a graph of the data given in Table 1. It is unlikely that a simple empirical relationship exists between film-speed and granularity: each unknown emulsion should be measured, at least until the manufacturer quotes some kind of granularity coefficient. However, one is tempted to deduce from the sparse data given in Fig. 9 that, when the emulsions are used in a given low-bandwidth system, the transferred noise-power is roughly proportional to the arithmetical film-speed rating. Or, less cautiously perhaps, that signal-to-noise ratio may be exchanged for film-speed at a rate not exceeding one decibel per degree (B.S. logarithmic).

TABLE 1

Emulsion	Rated film-speed† (Tungsten illumination)		Measured Wiener spectrum (mean level 0 to 20 cycles/mm) (square microns)
	A.S.A.	B.S.	
Ilford Pan.F	16	23°	0.10
Kodak Plus-X	64	29°	0.14
Kodak Tri-X	250	35°	0.555
Ilford H.P.S.	320	36°	0.62

† Earlier speed ratings (prior to the revised indices)

5. Film Processing

5.1 Variation of Signal-to-noise Ratio with Density

Thus far we have obtained, from the initial grain Wiener spectrum, the magnitude and spectrum of the noise after filtering and equalization (but prior to any gamma correcting circuits) by considering a scanned area of given optical density. Clearly, in addition, it is important to know how the output signal-to-noise ratio will vary with the optical density of the film. The variation in the shape of the noise-power spectrum (Wiener spectrum) with density is negligible and need not be considered. Before discussing the problem it is necessary to mention four somewhat different methods of using film in television applications. The film record placed in a film scanner or telecine may be one of the following:

* Eastman IIB control gamma = 0.65. The Pan.F results are interpolated from measurements on samples developed to other gammas.

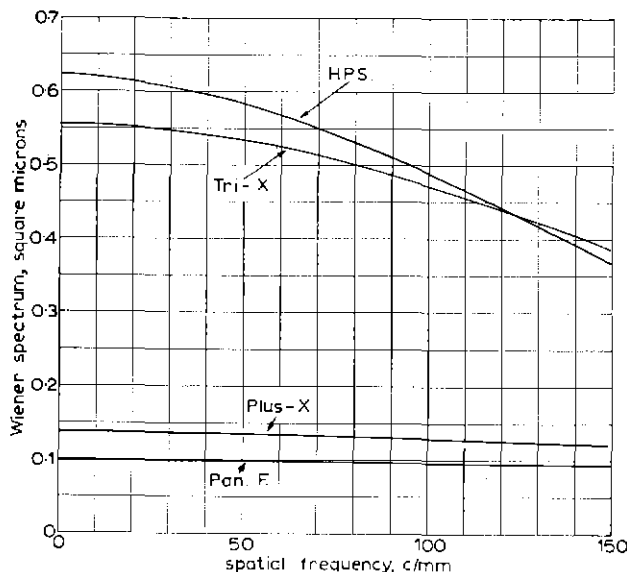


Fig. 8 — Measured Wiener spectra of four negative-type emulsions

- (I) A direct-positive record, e.g. as obtained from a film telerecording or cablefilm in those cases where a negative image is displayed.
- (II) Ordinary positive record, i.e. optically printed from a negative film record (or 'dupe' negative).
- (III) Reversal positive record—obtained by reversal processing.
- (IV) Negative record—the electrical signal being subsequently converted into its reciprocal and followed by appropriate gamma correction.

Better or worse comparison of these methods should be judged in terms of the granularity of the picture finally displayed, and this is dealt with in a later section. Suffice it to say, here, that at the photomultiplier output, prior to any non-linear transfer stages, methods (I) and (IV) have the same variation of mean signal-to-r.m.s. noise ratio with optical density. This variation is given, approximately, by

$$\frac{S}{N} \approx k \cdot D^{-0.6} \quad (4)$$

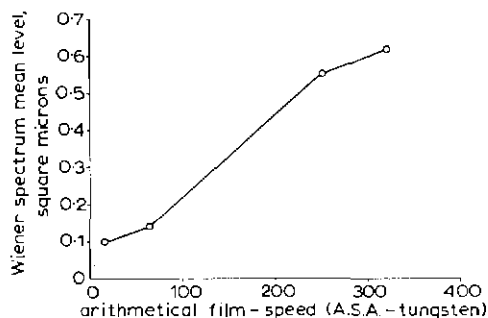


Fig. 9 — Relationship between rated film-speed and measured Wiener spectrum

where S is the mean signal level

N is the r.m.s. noise due to granularity

D is the optical density (above base)

k is a constant for a given emulsion and scanning aperture.

Deductions from recent granularity measurements on a range of Eastman Kodak emulsions, reported by Higgins and Stultz,⁶ suggest that the exponent in equation (4) may be closer to -0.4 . The value of the exponent is slightly dependent on the type of emulsion and its development gamma. However, for most practical purposes, equation (4) can be applied conveniently to a wide range of emulsions.

In method III above, where the positive record is prepared by a chemical reversal process, a similar variation law applies, but the exponent value is expected to be numerically greater (-0.6 to -0.7 say) because of the 'inverted' relationship between effective grain size and density associated with this method of processing.

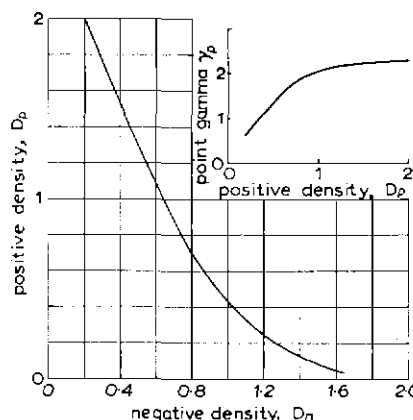


Fig. 10 — Typical development characteristics of a printing process

The variation of density which occurs in ordinary positive records, method II, cannot be quite so explicitly stated because, normally, the main component of the total granularity of the positive is that transferred from the negative during optical printing. The transferred component is modified by the (non-linear) transfer characteristic of the printing process. However, using a simplified theory of granularity transfer in low-bandwidth systems, it may be shown that the corresponding variation law takes the form

$$\frac{S}{N} \approx k' \left(a^2 \dot{\gamma}_p^2 D_n + c^2 D_p \right)^{-0.5} \quad (5)$$

where D_n and D_p are the conjugate densities of the negative and positive respectively.

(See, for example, Fig. 10.)

$\dot{\gamma}_p$ is the slope at the density D_p of the characteristic development curve of the positive emulsion (i.e. point-gamma).

a and c are constants proportional to the mean grain diameters of the developed negative and positive emulsions respectively.

k' is a constant depending on the equivalent scanning aperture.

D_p is related to D_n by the transfer characteristic of the particular printing process which, in turn, is determined by the exposure, the development time, and the developer, to mention but a few of the important factors. In general, the relation is not readily given by a simple empirical formula but the transfer characteristics shown in Fig. 10 are typical of those achieved in negative-positive processing. In this figure, which refers to Kodak 5302, a commonly used release printing emulsion, positive density D_p is plotted against negative density D_n (above base): it is arbitrarily assumed that a negative density of 0.2 gives rise to a positive density of 2.0. Inset in Fig. 10 is a second graph showing the point gamma, γ_p , of the development curve as a function of the density D_p , of the positive.

Equations (4) and (5) are illustrated by the curves labelled I and II respectively in Fig. 11, where relative

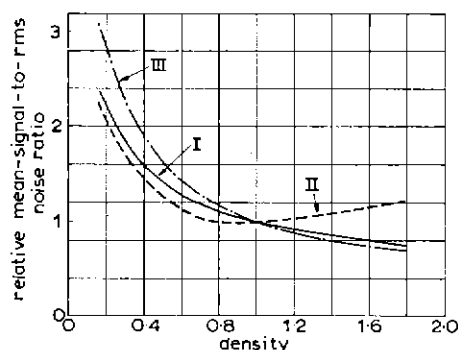


Fig. 11 — Variation of signal-to-noise ratio with optical density

- I Direct-positive
- II Ordinary positive
- III Reversal positive

mean-signal-to-r.m.s. noise ratio is plotted against density. Curve III in this figure is the relation given by equation (4) but with an exponent value of -0.65 . The values of the parameters taken for the evaluation of curve II from equation (5) are those given in Fig. 10, and that $a = 2c$. The variation shown by curve II is with respect to D_p . The three curves are normalized to unity at unit density. It will be seen from Fig. 11 that in each method (I, II, III) the signal-to-noise ratio increases rapidly as the lower densities are approached. Thus, even at this stage, one can immediately appreciate the well-known fact that the least-grainy film reproductions are obtained when the highlight or peak-white densities are of low value. It should be pointed out, however, that a low peak-white density usually results in some tonal distortion of the highlights; the effect of correction for such distortion is discussed later in this report.

5.2 Effect of Development Gamma

Commercial film-processing laboratories have standard, proven, techniques for exposing and developing positive-type emulsions. The print is, normally, developed to a high gamma (2.2 to 2.5) and the negative is therefore required to be developed to a low gamma (≈ 0.65) in order to achieve good overall tone reproduction. From the point of view of objective tone reproduction⁷ in photographic projection, a point gamma product ($\gamma_n \cdot \gamma_p$) equal to unity over a density range of about 2.0 would be ideal. In film tele-recording, where the tonal characteristics of the picture displayed for recording are largely under the control of the recording engineer, the choice of process gamma for the negative (or positive if the direct-positive method is being used) is somewhat less restricted. Film granularity is one of the several factors which may influence the actual gamma selected for a particular emulsion and method.

It is well known that increasing the development gamma of a negative-type emulsion leads to an increase in the average grain size. Recent experiments by the writer indicate that, for a given developed density, the mean grain diameter is approximately proportional to the square root of the point gamma achieved at that density. This relation is not expected to hold for positive-type (high gamma) emulsions, where the 'spread' of developed grain sizes with respect to the mean size is small. Using this experimental result in equation (5) above, by writing for ' a ',

$$a \approx a'(\gamma_n)^{0.5}$$

where γ_n is the point gamma of the negative at the density, D_n , we obtain

$$\frac{S}{N} \approx k' \left(a'^2 \gamma_p^2 \gamma_n D_n + c^2 D_p \right)^{-0.5} \quad (6)$$

Now, except for the 'toe', the transfer characteristic between D_p and D_n can be described by the approximation

$$\gamma_p D_n \approx \hat{D}_p - D_p \quad (7)$$

where \hat{D}_p is the positive density corresponding to zero negative density. Substituting (7) in the relation (6) gives

$$\frac{S}{N} \approx k' \left[a'^2 \gamma_p \gamma_n (\hat{D}_p - D_p) + c^2 D_p \right]^{-0.5} \quad (8)$$

This relation clearly indicates that, for a given print density, the mean-signal-to-r.m.s. noise ratio depends on the gamma product, $\gamma_n \cdot \gamma_p$. Now, if the overall photographic process is required to be substantially linear a necessary condition is that $\gamma_n \cdot \gamma_p$ should be close to unity over the density range of interest. In this instance, we see from equation (8) that the overall granularity is then independent of the process gamma achieved in negative or positive development. The above conclusions are in agreement with those obtained from direct experiment by other workers.*

Thus far, it has been tacitly assumed that the mean grain diameter of the positive-type emulsion used for the print is substantially independent of the development characteris-

* See reference 7, pp. 867-8.

tic: even if this is not so the mean grain diameter of the printing emulsion is usually somewhat less than that of the negative so that the second term in the square brackets in equation (8) is the least significant over most of the density range. Suppose, however, that the same type of emulsion can be used both for the negative and its positive print (as, for example, with the 16-mm telerecording emulsion, Kodak 8374). In this case, 'c' is now commensurate in value to 'a' in equation (8), and if we assume as before that

$$a \approx a'(\dot{\gamma}_n)^{0.5}$$

and write, correspondingly,

$$c \approx a'(\dot{\gamma}_p)^{0.5}$$

then equation (8) becomes

$$\frac{S}{N} \approx \frac{k'}{a'} \left[\dot{\gamma}_n \dot{\gamma}_p (\hat{D}_p - D_p) + \dot{\gamma}_p D_p \right]^{-0.5}$$

Thus, in this situation, it is preferable to use a high value of gamma for the negative and a low value for the print rather than vice-versa, because, for a given value of D_p , the signal-to-noise ratio decreases as $\dot{\gamma}_p$ increases.

In direct-positive telerecording, when a negative-type emulsion is used for the positive record, it would appear advantageous to keep the development gamma as low as possible.

6. Signal Processing

Normally, the video signal output of a film scanner is corrected by non-linear amplification so that, applied to an ordinary display tube ideally adjusted and viewed, an approximately linear correspondence between the optical transmission of the film and the displayed luminance is achieved. An obvious exception occurs when a negative record is placed in the scanner; here, the 'reciprocating' effect automatically achieved in optical printing must be simulated electronically. In a general analysis, it is convenient to assume initially that overall linearity exists and later, perhaps, to consider the subjective effects of factors which may modify the linearity. This procedure allows the electrical transmission path to be circumvented: the granularity can then be discussed immediately in terms of the resulting luminance perturbations of the displayed picture. A proviso is that the signal-to-r.m.s. noise ratio is everywhere reasonably high.

Since, however, electrical measurements are often carried out at a non-linear point in the transmission path, e.g. at the receiver input, it seems worth noting briefly the main effects of a non-linear transfer characteristic of the power-law type, on the magnitude of the signal-to-noise ratio and on the variation of the latter with film density.

Suppose that the relative magnitudes of the signal at two points, A and B say, are related by the equation

$$S_B = (S_A)^n \quad 0 \leq S \leq 1 \quad (9)$$

where S_A and S_B are the normalized signal values at A and B respectively, and n is any constant. It is readily shown that the corresponding signal-to-r.m.s. noise ratios $(S/N)_A$ and $(S/N)_B$ are simply related by the approximation

$$\left(\frac{S}{N}\right)_B \approx \frac{1}{n} \cdot \left(\frac{S}{N}\right)_A \quad (10)$$

The degree of approximation depends on the value of N compared with S , and on the value of n . It is assumed, of course, that the path A to B does not include any significant sources of noise. It will be seen from equation (10) that the variation of S/N with density is not altered by this type of non-linearity but the magnitude is everywhere multiplied by the reciprocal of the exponent, n . Thus, for example, when $n > 1$ the measured mean signal-to-r.m.s. noise ratio, for a given density of film, is less at point B than at point A.

In practical measurements, the r.m.s. noise voltage is often referred to that of the peak (picture) signal, i.e. black-to-white voltage. Rewriting equation (10) in terms of the peak-signal-to-r.m.s. noise ratio $(1/N)_B$ and $(1/N)_A$ (remembering that, by definition, peak-signal equals unity), and using equation (9) we obtain

$$\left(\frac{1}{N}\right)_B \approx \left[\frac{S_A^{(1-n)}}{n}\right] \left(\frac{1}{N}\right)_A \quad (11)$$

The scaling factor in the square brackets in equation (11) is simply the reciprocal slope of the transfer characteristic at the signal value S_A . The purpose of putting the relationship in the above form is to emphasize two useful features which may be exploited in practical scanner-noise measurements. The first is that if n is known, S_A can always be selected so that $S_A^{(1-n)}/n$ equals unity: the peak signal-to-r.m.s. noise ratio at point A then equals that at point B. If, for example, point A is the photomultiplier output of a flying-spot film scanner then S_A varies directly with the mean transmission of the film (relative to the peak-white transmission) and equation (11) becomes,

$$\left(\frac{1}{N}\right)_B \approx \left[\frac{t^{(1-n)}}{n}\right] \cdot \left(\frac{1}{N}\right)_A$$

where t is the transmission of the film. In terms of optical density it can be shown that unity scaling factor occurs at a density D_1 , given by

$$D_1 = \frac{\log_{10} n}{n-1}$$

A second feature of equation (11) is that another value of S_A can be selected such that the rate of change of the scaling factor $S_A^{(1-n)}/n$ with n is zero. This condition is useful when the random electrical-noise levels of different flying-spot scanners are being compared by measurements at a non-linear point:* here, the nominal value of n is known but the actual values may vary between different scanners.

The zero-rate-of-change condition occurs at the value S' given by

$$\log_{10} S' = \frac{-0.434}{n}$$

* The author is indebted to Mr C. B. B. Wood, for pointing out this condition and its practical value.

A typical nominal value of n is 0.4, so that if noise measurements are carried out at $S'_x \approx 0.1$ the error introduced by unknown (small) variations of n is a minimum, and over the range 0.35 to 0.45, say, it is negligible.

7. Displayed Granularity

It is not difficult to estimate the statistical magnitude and Wiener spectrum of the luminance perturbations resulting from random variations of the input signal due to granularity. It is more difficult to predict the final assessment of the displayed granularity in terms of subjective annoyance and tolerance.

In this analysis, which is concerned with relatively large picture areas having substantially uniform luminance, the displayed granularity is objectively specified in terms of the ratio of the r.m.s. deviation of the luminance from its mean value to the mean luminance. The luminance perturbations may be regarded as spatial variations for one complete scan of the picture area. The displayed granularity is thus considered to be 'frozen' and, in some respects, similar to the graininess of an ordinary photographic print. One might object fairly to this static viewpoint, on the grounds that television is mainly concerned with motion pictures; so that with cine-film, for instance, the luminance of any point in the displayed picture is randomly time-modulated by the frame-to-frame granularity. Further, because the storage time of the eye is somewhat greater than the normal television picture period (i.e. >33 to 40 ms), subjective visual differences between static and dynamic forms of displayed granularity can be expected:^{8,9} the dynamic form is, in general, less visible than the static form for a given input signal-to-noise ratio. To allow for these differences the assessment of the relative visibility of the displayed film granularity attempted here is based on visibility thresholds of perceptibility and annoyance determined from the results of subjective tests using dynamic random noise (electrically generated) having a uniform noise-power spectrum.

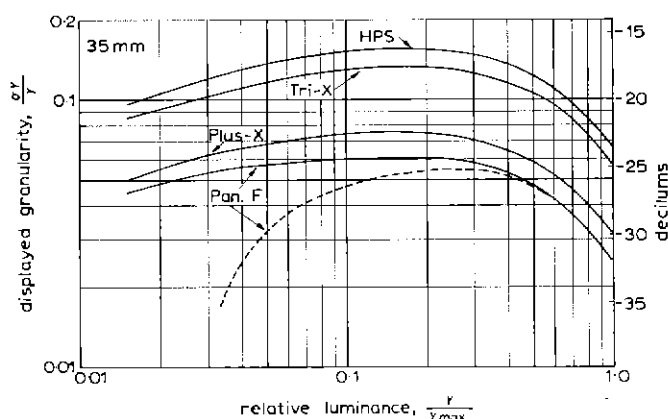


Fig. 12 — Displayed-granularity curves: negative-to-positive process

— Unlimited picture contrast ratio
 - - - - - 50 : 1 picture contrast ratio

7.1 Granularity Distribution Curves

7.1.1 Negative-to-positive Process (Method II, Section 5.1)

Using the measured granularity results for the four negative-type, 35-mm, emulsions already given (Fig. 8), we obtain the displayed-granularity data shown in Fig. 12 where the ratio of the r.m.s. deviation in luminance to the mean luminance ($\sigma Y/Y$) is plotted against the relative luminance (Y/Y_{max}) using logarithmic co-ordinate scales. The quantity $\sigma Y/Y$ is a ratio of luminances corresponding to the r.m.s. noise-to-mean-signal ratio in the electrical sense. Following Mertz,¹⁰ $20 \log_{10}(\sigma Y/Y)$ is here called a 'decilum' measure to denote that a ratio of luminances is involved. A decilum scale is shown on the right in Fig. 12. In deducing the curves shown in Fig. 12 (and, where appropriate, in Figs. 13, 14, and 15) the following conditions were assumed:

1. Overall film-to-picture linearity.
2. The negative-type emulsions are optically printed on Kodak 5302 positive-type emulsion. The printing frequency response characteristic is taken to be that given by Lamberts¹¹ for this emulsion, the development characteristic is as shown in Fig. 10, and the Wiener spectrum of uniform magnitude (equal to 0.04 square microns at a density of 0.5 above base).
3. Peak-white luminance of the picture corresponds to a positive density of 0.2 above base.
4. Negative density of 0.2 (above base) prints to a positive density of 2.0.
5. Video bandwidth limit corresponding to 13 cycles/mm for 35-mm gauge film and 28 cycles/mm for 16-mm gauge.
6. In the absence of video equalization and the bandwidth limiting filter, the equivalent scanning aperture of the whole system (including the display-tube scanning spot) is assumed to have a Gaussian frequency response characteristic which is 1.5 dB down at 13 cycles/mm and 6 dB down at 28 cycles/mm.

The curves shown in Fig. 12 refer to 35-mm gauge film (25.15-mm diagonal format). To obtain corresponding data for 16-mm gauge working, under the condition specified above, add 1.5 decilums to the ordinate values if the channel response is not equalized or 4 decilums if fully aperture-corrected in the line direction.

The dashed-line tail to the lower curve in Fig. 12 shows the effect on the displayed granularity of a steady ambient illumination of the display tube,¹² and/or uniform tube flare, reducing the maximum available contrast ratio of the picture to 50:1.

7.1.2 Direct-positive Process (Method I, Section 5.1)

In this process negative-type emulsions are sometimes used, but developed to a higher gamma than when used in a negative-positive process in order to maintain an adequate contrast range. The displayed 'negative' picture in the recording process may be pre-distorted in tonal value to counteract the photographic non-linearity. Fig. 13(a) and (b) shows displayed-granularity curves deduced for a 35-mm film (Ilford Pan.F) and a 16-mm film (Kodak

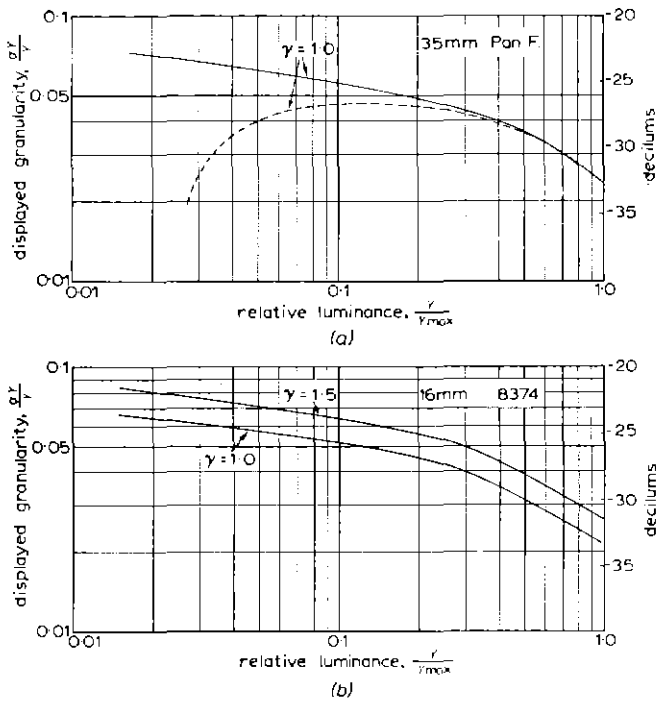


Fig. 13 — Displayed-granularity curves:
direct-positive process
— Unlimited picture contrast ratio
- - - 50 : 1 picture contrast ratio

8374) respectively, when used in a direct-positive process. In Fig. 13(a) the dashed-line curve refers, again, to the 50:1 contrast-limited condition of the display tube. The upper curve in Fig. 13(b) shows the estimated increase in film granularity if the emulsion (Kodak 8374) is developed to a gamma of 1.5 instead of 1.0.

Again, the assumptions given in the preceding section were used, with the exception of (2) and (4) which do not apply.

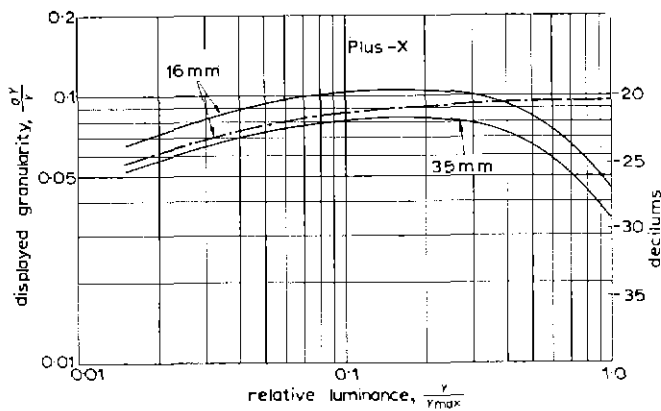


Fig. 14 — Displayed-granularity curves:
direct-negative process
— No correction for photographic non-linearities
- - - Full electronic post-correction of photographic non-linearities

7.1.3 Direct-negative Process (Method IV, Section 5.1)

Here, the negative is exposed and developed as for an ordinary negative-to-positive process but, in the interest of time, the negative record may be placed in a scanner and transmitted prior to optical printing. The full lines in Fig. 14 show displayed-granularity curves for a negative record, deduced by assuming that the development characteristics of a standard printing emulsion are simulated electronically. The chain-line curve in the figure shows the effect of 'full' post-correction of the signal by which the photographic non-linearities are eliminated. In telerecording, such non-linear correction (black and white stretch) can be achieved approximately by pre-distortion of the picture displayed in the telerecording machine, but this does not affect the film granularity, although it may well increase the level of noise due to other causes.

The data shown in Fig. 14 refer to Kodak Plus-X, developed to a gamma of 0.65; the film gauge sizes to which the granularity curves refer are indicated on the figure.

7.1.4 Reversal Process (Method III, Section 5.1)

Unfortunately, granularity or Wiener spectrum measurements were not carried out on emulsions intended for reversal processing. However, using the relationship given by equation (4), in Section 5.1, with an exponent value of -0.65 , a displayed-granularity curve was deduced assuming that Kodak Plus-X is used as the reversal emulsion. The tentative result is shown in Fig. 15: the dashed-line 'tail' refers to the 50:1, contrast-limited condition of the display tube.

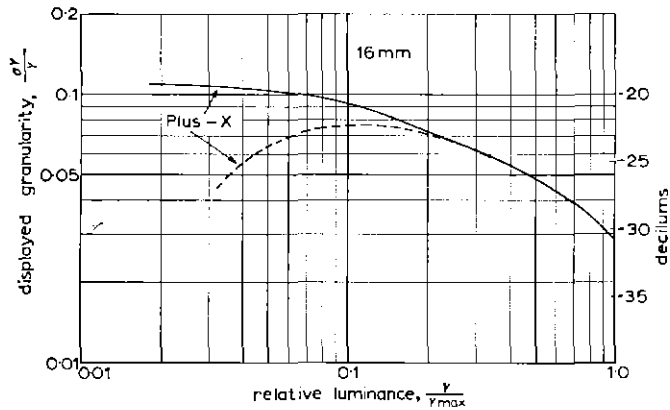


Fig. 15 — Displayed-granularity curves:
reversal process
— Unlimited picture contrast ratio
- - - 50 : 1 picture contrast ratio

7.1.5 Effect of Over-exposure

The general increase in granularity due to over-exposure, leading to abnormally high average densities, is well known. As a quantitative example, the displayed granularity deduced for a normal exposure, an over-exposed negative, and an over-exposed positive are shown in Fig. 16 by the curves labelled (a), (b), and (c) respectively.

The data shown in the figure refer to the Pan.F, 35-mm, emulsion used in an ordinary negative-to-positive process (see Section 7.1.1). Curve (a) is for a normal exposure and is, in fact, that already given in Fig. 12. Curve (b) refers to the condition where the negative record is over-exposed by a factor of two; in this instance the average density of the negative is assumed to be increased by approximately 0.2. Curve (c) is the condition where the positive emulsion is over-exposed by a factor of two, leading to a peak-white density of 0.5 above base.

7.2 Granularity Spectrum

In the direction of scan, the form of the (Wiener) spectrum of the displayed granularity is that given by the product of the original grain Wiener spectrum with the squared modulus of the overall frequency response function of the television channel, including the final display tube. At right angles to the direction of scan (and in other directions to a diminishing extent), the spectrum is somewhat differently modified because of the finite line-density of the normal television scanning process. As indicated in the Appendix (Fig. 20(g)), the spectrum in this direction may have a quasi-periodic structure in contradistinction to the smoothly decreasing characteristic of the original spectrum. Perhaps of greater importance, from a subjective standpoint, are the added spectral 'spikes' due to the fundamental and harmonic sine-wave components of the scanning-line structure representing the mean luminance level, i.e. even in the absence of the random granularity. The prominence of the added spectral 'spikes' depends on the size and form of the display-tube scanning spot, and on the luminance level relative to that of peak-white. Thus in the lighter tones of the picture the scanning-line structure may be sufficiently apparent to mask the visual effect of the random granularity in this direction. Too little experimental evidence is available, concerning the grain-masking effect of the displayed scanning-line structure, to allow a quantitative discussion of this point.

8. Subjective Assessments

It is beyond the scope of this monograph to attempt a comprehensive review of the subjective factors involved in the assessment of the visibility of the displayed granularity. Some important factors are briefly discussed.

8.1 Visual Thresholds

Clearly, in order to interpret fully the displayed-granularity data given in Figs. 12 to 16, we must compare them with an appropriate threshold curve expressed in the same terms, i.e. $\sigma Y/Y$ as a function of the relative luminance Y/Y_{max} . Not unexpectedly, experience with steady photometric fields has shown that visual contrast thresholds cannot be specified uniquely in terms of physical measures of the stimuli: there is 'one threshold for every situation' so to speak. The just-perceptible brightness contrast between two adjacent fields, for instance, depends on their absolute luminance, exposure, area, boundary sharpness, luminance distribution of the surrounding field, to mention some of the influential physical factors.

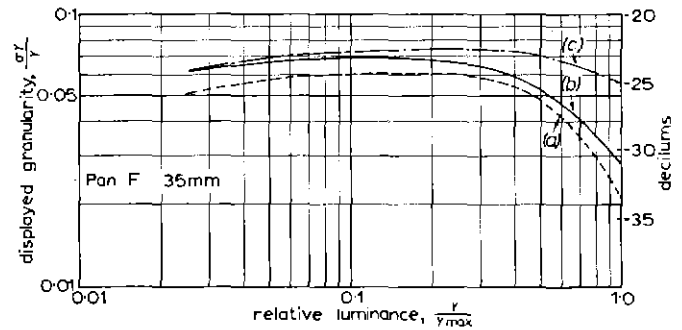


Fig. 16 — Displayed-granularity curves: effect of over-exposure

- (a) Normal exposure
- (b) Over-exposed negative
- (c) Over-exposed positive

ance distribution of the surrounding field, to mention some of the influential physical factors.

The peak-white luminance of normal domestic television receivers is of the order of 20 ft-Lamberts, and the picture-contrast ratio is not usually greater than 50:1. Hence, in television, the luminance range to be considered is substantially invariant. Also, the equivalent adaptation level¹³ of the picture is restricted to roughly the same range, because the adaptation level is determined largely by the luminance distribution of the immediate surroundings to the particular area of interest in a given picture. Since the eye is free to wander over the whole picture, a reasonable assumption is that the equivalent adaptation level is given by the average luminance of the whole picture: thus a high-key scene would produce a high adaptation level and, likewise, a low-key scene a low adaptation level.

Recent experiments^{8,14} have shown that the variation of the noise-visibility threshold with luminance level in a television display is different from that predicted from photometric studies of the variation of the luminance-contrast threshold (i.e. Fechner fraction $\Delta Y/Y$) with luminance. In general, the threshold for temporally-in-

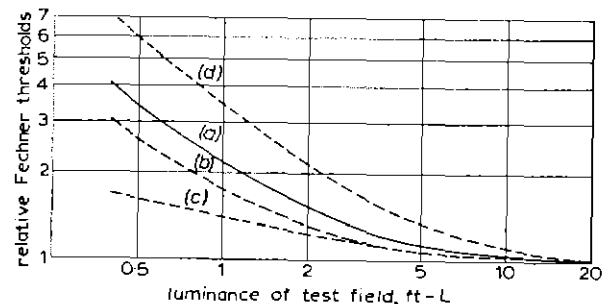


Fig. 17 — Relative Fechner thresholds for photometric fields and television noise

- (a) Television random noise
- (b) Photometric threshold (5 ft-L equivalent adaptation)
- (c) Photometric threshold (minimum adaptation)
- (d) Photometric threshold (maximum adaptation)

coherent random-noise in a television display (50 fields/sec interlaced) increases with decreasing luminance at a faster rate than the Fechner threshold for steady photometric displays, all other factors remaining constant. For example, the full-line curve (a) in Fig. 17, shows the form of the visibility threshold obtained by Newell and Geddes⁸ for random fluctuation noise in a television display (U.K. standards) having a peak-white luminance of 20 ft-L, and exhibiting a special test-card picture of average background luminance equal to 5 ft-L, approximately. For comparison the dashed-line curve shown at (b) is the Fechner contrast threshold predicted by the empirical formulae given by Moon and Spencer¹³ for the same luminance range, and an equivalent adaptation level equal to 5 ft-L. Logarithmic co-ordinate scales are used in the figure and the ordinate values are the relative (fractional) increase in stimulus for constant visibility, normalized to unity at the peak-white luminance. Also indicated in Fig. 17, at (c) and (d), are the expected limits of the threshold for minimum and maximum equivalent adaptations respectively, according to the Moon and Spencer formulae. It will be seen that the differences in the visibility thresholds which appear to exist, at the lower luminance levels, between the optical and television displays are considerably smaller than the possible changes with adaptation conditions.

The absolute values of noise-visibility thresholds have been determined subjectively for television displays, using both pictures and test patterns, by a number of workers;^{15,16,17} but mainly in terms of the signal-to-noise ratio at the input to the display. The transfer characteristics of the particular display tubes, in the condition used for the

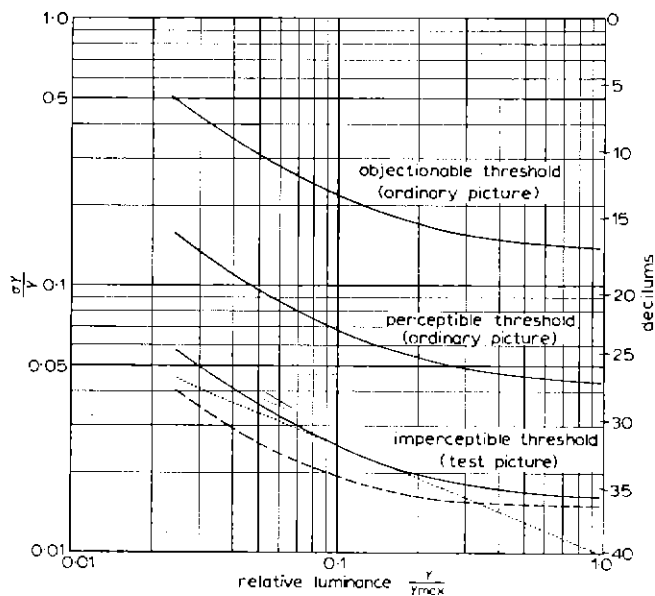


Fig. 18 — Absolute threshold curves of perceptibility and annoyance

- Wide-band (uniform-spectrum) television random noise
- - - - - Optical Fechner threshold, $\Delta Y/Y$
- Luminance noise distribution due to noise added at monitor input

experiments, must, however, be known in order to deduce accurately the corresponding thresholds in terms of the displayed luminance variations. Further, the experiments were carried out using electrically-generated noise (usually added at the monitor input) which has a somewhat different quantitative distribution over the grey-scale than that originating from film-grain, even though the character and appearance of the displayed granularity from each cause may be similar.

There seems to be substantial agreement that for electrical random noise having a wide (0 to 3 Mc/s) and uniform noise-power spectrum, added at the display-tube input, a just-not-perceptible threshold lies close to a peak-signal-to-r.m.s. noise ratio of 48 decibels. This result, obtained by Kilvington *et al.*,¹⁵ can be expected when viewing, at a distance of four times the picture height, a test picture such as several broad vertical stripes each of different luminance arranged to cover the available grey-scale. Assuming that the display-tube has a power-law transfer characteristic with an exponent of 2.5, the granularity distribution over the grey scale can be deduced.^{10,12} The result, for an input noise level of -48 decibels relative to peak signal, is indicated by the dotted line in Fig. 18. Now, since the relative variation of the visual threshold over the grey scale for random noise is known (curve (a) in Fig. 17), an absolute visibility threshold can be established by supposing that the curve is tangential to the added-noise distribution (i.e. tangential to the dotted-line in Fig. 18). The result is shown by the curve labelled 'imperceptible threshold' in Fig. 18. The term imperceptible is used here because the subjective criterion used in the original experiment¹⁵ was the input noise-level at which the noise was 'just-not-visible' in contradistinction to 'just visible'. The lower (dashed-line) curve in Fig. 18 is the corresponding optical (photometric, static) Fechner threshold, $\Delta Y/Y$, for equivalent viewing conditions. The close proximity of the imperceptible threshold for television noise to the Fechner threshold $\Delta Y/Y$ for uniform photometric fields is most interesting. It suggests, in fact, that the root-mean-square measure (in contradistinction to, say, the peak-to-peak measure) of the spatial fluctuations in luminance caused by random-noise is visually equivalent, at least approximately, to the simple incremental measure of the difference in luminance between two juxtaposed fields of uniform luminance. In other words, the 'd.c.' equivalence of the r.m.s. measure, fundamental to fluctuating electrical currents, appears to hold also for brightness-contrast perception.

8.2 Visual Sensitivity

The type of threshold discussed above can be regarded as the limit of visibility under rather critical viewing conditions. It is, therefore, an unrealistic threshold against which to assess the displayed-granularity examples shown in Figs. 12 to 16. A less critical threshold is afforded, for example, by the work of Weaver¹⁶ which, in addition, gives a valuable estimate of the sensitivity of the average observer to luminance noise. Briefly, Weaver added random-noise to the input of a television monitor (exhibiting a

typical outdoor scene) and asked observers to assess the degree of its visibility or annoyance according to the six-point scale,

Grade	Criterion
1	Imperceptible
2	Just-perceptible
3	Definitely perceptible— but not disturbing
4	Somewhat objectionable
5	Definitely objectionable
6	Unusable

A statistical analysis of the results showed that, for both 405- and 625-line standards and two types of noise, the average sensitivity to luminance noise was approximately 3 dB per lumen.* In less sophisticated terms, the sensitivity can be expressed as 5 dB per grade using the above six-point scale. This result has recently been confirmed by Newell and Geddes¹⁷ in a similar subjective experiment.

The two upper threshold curves shown in Fig. 18, are derived from the mean of the results for both scanning standards given by the above experiments for added uniform-spectrum noise. (The bandwidth of the added noise was limited to approximately 3 Mc/s for the 405-line standard, and 5 Mc/s for the 625-line standard.) The threshold termed 'perceptible' corresponds to a mean-grading of 2.0, and that termed 'objectionable' corresponds to a mean-grading of 4.0; both thresholds are expressed in terms of the relative r.m.s. luminance deviations required, and a decilum scale is shown on the right of the figure.

8.3 Displayed Granularity

In general, a threshold of given perceptibility or annoyance has been shown^{9,15} to depend on the bandwidth of the signal and, to a smaller extent, on the manner in which the electrical noise power is spectrally distributed over the band. For example, noise with a triangular or up-tilted spectral distribution is less visible than noise of uniform spectrum having the same total noise-power at the input. This is explained by the fact that, at a constant viewing distance, the effective spectral weighting of the perceived noise, due to the drooping frequency-response characteristic of the eye (and the display-tube scanning aperture), is substantially greater for noise whose energy is concentrated towards the higher-frequency components.

Finally, an important law reported by Mertz,¹⁰ is that the visibility of random noise in a television channel is independent of the video bandwidth providing that the spectral density of the electrical noise-power remains uniform and constant within the band. The fundamental significance of this effect, which was discovered experimentally by H. W. Baldwin,¹⁰ does not appear to have been fully investigated. Consequently, the partial bearing the effect may have on the perception of other types of noise of, say, non-uniform spectral distribution, remains uncertain.

* Psychometric unit defining a measure of observer reaction such that 50 per cent of observers would notice the change in picture impairment.

8.4 Numerical Examples

If a granularity distribution curve, relating to a given film process using a particular emulsion, is compared with the absolute thresholds shown in Fig. 18, a quantitative estimate of the perceived granularity is readily obtained. In Table 2, for example, the maximum excursion of each of the displayed-granularity curves shown in Figs. 12 to 16 above the 'perceptible' threshold is given in decilum units. Also included in the Table are the corresponding estimated subjective mean-gradings and the relative luminances at which the granularity is most visible.

It is assumed that the viewing conditions are such that the maximum available picture contrast ratio is 50:1. Results are given for both 35-mm gauge and 16-mm gauge film (see Section 7.1.1).

All the values shown in Table 2 refer to the particular equivalent scanning aperture defined in Section 7.1.1. Clearly, if other equivalent scanning apertures are used different values may be obtained. An estimate of the probable variation with aperture is afforded by the data given in Fig. 7.

If full video equalization is achieved in the scanning-line direction, approximately 2.0 decilums (0.4 subjective grade) should be added to the values shown for 16-mm gauge working.

TABLE 2

Film Process and Emulsion Type	Maximum Excursion above Perceptible Threshold (Decilum units)		Estimated Mean Grading (Six-point Scale)		Luminance for Maximum Visibility
	35-mm	16-mm	35-mm	16-mm	% of Peak-White Luminance
<i>Negative-Positive</i>					
Pan.F/5302	1.0	2.5	2.2	2.5	35
Plus-X/5302	2.5	4.0	2.5	2.8	35
Tri-X/5302	7.5	9.0	3.5	3.8	35
HPS/5302	9.0	10.5	3.8	4.1	35
<i>Negative-Positive</i>					
Pan.F/5302					
(a) Normal exposure	1.0		2.2		35
(b) Over-exposed negative	2.0		2.4		35
(c) Over-exposed positive	3.5		2.7		50
<i>Direct-Positive</i>					
Pan.F ($\gamma=1.0$)	-1.5	0.5	1.7	2.1	25
8374 ($\gamma=1.0$)		-2.0		1.6	25
8374 ($\gamma=1.5$)		0.0		2.0	25
<i>Direct-Negative</i>					
Plus-X	3.5	5.5	2.7	3.1	35
Plus-X (linearity corrected)	4.5	6.5	2.9	3.3	100
<i>Reversal</i>					
Plus-X ($\gamma=1.0$)	0.5	2.5	2.1	2.5	20

9. Conclusions

The photographic process has been so extensively studied and so diversely applied that some of the conclusions

reached in this simplified analysis may only serve to reaffirm features already well known to users of film in television either by their experience or by the previous researches of others.

However, to conclude, some specific points of interest in the television applications of cine-film are summarized: the values mentioned refer, of course, to a typical television broadcasting system.

1. In a conventional, 35-mm, negative-to-positive process using the finer-grained but slower negative emulsions, such as Plus-X and Pan.F., the displayed-granularity is only slightly above the perceptible threshold associated with ordinary pictures and good viewing conditions (mean-grading of 2.0). The same emulsions used in 16-mm gauge will still be acceptable although up to 0.8 subjective grade worse depending on the equivalent scanning aperture of the system. Use of the faster negative emulsions, such as Tri-X or HPS, is expected to result in a granularity category slightly below the annoying or objectionable threshold (mean-grading of 4.0). As before, 16-mm gauge working is likely to be up to 0.8 subjective grade worse than 35 mm.

2. Over-exposure of either the negative or positive or both results in an increase in the displayed granularity. The increase is greater for an over-exposed positive because of the corresponding increase in the average transfer gamma of the print in the highlight region of the record. Typical figures, for an over-exposure factor of two, are one decilum (0.2 subjective grade) increase for the negative and 2.5 decilums (0.5 subjective grade) increase for the positive.

3. In the displayed picture the tonal region most sensitive to film-granularity is the mid-grey to light-grey region, with a maximum sensitivity centred at a luminance which is 20 per cent to 35 per cent of that of peak-white, depending on the film process and the maximum available contrast ratio of the display.

Any attempt to remove the inherent non-linearity of the photographic process in the highlights by post-correction of the signal (white stretch) results in a shift of the region of maximum sensitivity towards peak-white, in addition to increasing the granularity.

4. Direct transmission from a negative record, prepared as for normal printing, results in a small increase (of about 0.25 grade) in the displayed granularity compared with that obtained from a standard print of it. This increase, however, is associated with a better overall resolution because the normal loss of resolution due to the printing emulsion is eliminated.

5. In film telerecording, using the direct-positive method the displayed granularity can be kept below the perceptible threshold by the use of the finer-grained emulsions: this leaves room for some pre-correction of the non-linearities. It is preferable to keep the development gamma of these emulsions as low as possible consistent, of course, with the maintenance of an adequate contrast range.

6. For a given film-speed, the chemical reversal process affords a somewhat better resolution and less film grain than the negative-to-positive process. The results for one

emulsion (Plus-X), supposed to be used for both processes, suggest a reduction in the displayed granularity of approximately 2.0 decilums (0.4 subjective grade).

7. In a conventional negative-to-positive process the granularity of the print, at a given density, depends on the point-gamma product achieved at that density, rather than on the individual process gammas. Where the same type of emulsion can be used for both the negative and its print, as with certain television recording emulsions, there appears to be some advantage to be gained by keeping the negative gamma higher than the print gamma rather than vice versa.

8. In general, resolution can be traded for signal-to-noise ratio by modifying the equivalent scanning aperture of the system, e.g. by applying vertical spot-wobble or by the use of an electrical low-pass filter. How worth while such trading is, in terms of subjective picture quality, depends on the magnitude and spectrum of the granularity in a manner which is not entirely understood.

9. The diameter of the scanning beam in a film scanner should not be too small, unless spot-wobble is employed, because this may lead to a large increase in granularity for only a small increase in picture sharpness.

10. With ordinary negative-type emulsions, film-speed can be exchanged for overall signal-to-noise ratio at a rate which is expected to be not greater than one decibel per logarithmic degree.* Thus, for example, changing from one emulsion to another having twice the film-speed is likely to result in an increased picture impairment due to granularity, but not by more than 0.6 subjective grade.

10. Acknowledgments

The writer wishes to thank Mr C. B. B. Wood and Mr W. N. Sproson for helpful discussion of several points.

11. References

1. Schade, O. H., *The Grain Structure of Television Images*, J.S.M.P.T.E., Vol. 61, p. 97, August 1953.
2. Schade, O. H., *Image Analysis in Photographic and Television Systems*, J.S.M.P.T.E., Vol. 64, p. 593, November 1955.
3. Clark Jones, R., *New Method of Describing and Measuring the Granularity of Photographic Materials*, J. Opt. Soc. Am., Vol. 10, p. 799, 1955.
4. Monteath, G. D., *Vertical Resolution and Line Broadening*, BBC Engineering Division Monograph No. 45, December 1962.
5. Howorth, D., *An Experimental Vertical Aperture Corrector*, BBC Engineering Division Monograph No. 47, Part I, May 1963.
6. Higgins, G. C. and Stultz, K. F., *Experimental Study of r.m.s. Granularity as a Function of Scanning-Spot Size*, J. Opt. Soc. Am., Vol. 49, p. 925, 1959.
7. Mees, C. E. K., *The Theory of the Photographic Process*, Chapter XX, Macmillan, 1948.
8. *Visibility of Small Luminance Perturbations in Television Displays*, Newell, G. F. and Geddes, W. K. E., Proc. I.E.E., Vol. 110, No. 11, November 1963.
9. Maurice, R. D. A., Gilbert, M., Newell, G. F., and Spencer, J. G., *The Visibility of Noise in Television*, BBC Engineering Division Monograph No. 3, Part III, October 1955.

* B.S. logarithmic.

10. Mertz, P., **Perception of Television Random Noise**, J.S.M.P.T.E., Vol. 54, p. 8, January 1950.
11. Lamberts, R. L., **Sine-Wave Response Techniques in Photographic Printing**, J. Opt. Soc. Am., Vol. 51, p. 982, September 1961.
12. Hacking, K., **The Relative Visibility of Random Noise Over the Grey Scale**, J. Brit. I.R.E., Vol. 23, p. 307, April 1962.
13. Moon, P. and Spencer, D. E., **The Visual Effect of Non-Uniform Surrounds**, J. Opt. Soc. Am., Vol. 35, March 1945.
14. Billard, P., **Les Seuils Différentiels de Luminance en Télévision**, Optica Acta, Vol. 5 (Hors Série), p. 283, January 1958.
15. Kilvington, T., Judd, D. L., and Meatyard, L. R., **An Investigation of the Visibility of Noise on Television Pictures**, Post Office Engineering Department Radio Report No. 2289, 1954.
16. Weaver, L. E., **Subjective Impairment of Television Pictures**, Electronic and Radio Engineer, Vol. 36, No. 5, p. 170, May 1959.
17. Geddes, W. K. E., **The Relative Impairment Produced by Random Noise in 405-line and 625-line Television Pictures**, E.B.U. Review, Part A, No. 78, p. 46, April 1963.

APPENDIX

GRANULARITY TRANSFER IN A LINEAR SEQUENTIAL TELEVISION SYSTEM

Suppose that developed photographic film of uniform (macro) density is placed in the gate of a film scanner. Let the near-random spatial fluctuations of its transmission coefficient from point-to-point due to emulsion granularity be described by the autocorrelation function $\phi(k, l)$, defined as

$$\phi(k, l) \equiv \frac{1}{A} \iint_{(A)} t(x, y) t(x-k, y-l) dx dy - (\bar{t}_A)^2$$

where $t(x, y)$ is the transmission function of the film, x and y being rectangular co-ordinate axes lying in the plane of the film. The correlation function variables k and l correspond to the x and y co-ordinate directions respectively. A is an area of the surface, enclosing the origin of co-ordinates, and is supposed large compared with the region over which the point-to-point correlation of the transmission fluctuations are significantly non-zero. Further, it is assumed that the granularity is statistically stationary so that $\phi(k, l)$ is independent of the position of the origin of the (x, y) co-ordinates. (\bar{t}_A) is the mean transmission of the film over the area A . Less formally, we might suppose that the origin of co-ordinates is somewhere near the centre of the film-frame, and A is the area of the latter: measurements on ordinary emulsions show that A will then be substantially greater than the product (k_1, l_1) which defines the practical limits of the region of significant correlation.

The grain Wiener spectrum, $N(f_x, f_y)$, is defined by the Fourier transform of the autocorrelation function:

$$N(f_x, f_y) \equiv \iint_{(\infty)} \phi(k, l) e^{-2\pi i(kf_x + lf_y)} dk dl$$

where f_x, f_y are spatial frequency variables corresponding to the directions denoted by their subscripts. (The Wiener spectrum is analogous to the power spectral-density of electrical random-fluctuation noise.)

Let the film be scanned once in sequential parallel lines, lying in the x co-ordinate direction, with L lines per unit distance in the y direction. Figs. 19 and 20 illustrate some of the functions and their Fourier transforms relevant to the effects of the picture analysis and synthesis operations, respectively, in such a system.

At (a) in Fig. 19 is shown the autocorrelation function (main sections) of the film grain when the latter is convolved with the aperture function representing the spatial intensity distribution of the scanning beam. Let the aperture-modified autocorrelation function be $\phi'(k, l)$ and its Wiener spectrum be $N'(f_x, f_y)$. It may be shown that the (one-dimensional) autocorrelation function, $\phi''(\tau)$, of the fluctuations in the initial video picture signal is given by the plane sections $\phi'(k, n/L)$, where $n = 0, \pm 1, \pm 2, \pm 3, \dots$ equally spaced in time by the line-scan period T in the manner shown in Fig. 19(b). The spatial displacement co-ordinate k is, of course, reduced to the corresponding temporal displacement co-ordinate $\tau = k/v$, where v is the horizontal or line-scan velocity, in this operation. Moreover the autocorrelation function $\phi''(\tau)$ will have significant values in intervals of time which are much less than the line-scan period T , and therefore $\phi''(\tau)$ is comprised of relatively sharp pulses located at $\tau = 0, \pm T, \pm 2T, \dots$. It will be seen from Fig. 19(a) that the number and relative magnitudes of the pulses (other than the central pulse at $\tau = 0$) will depend on the line-density L , in relation to the extent and magnitude of the function $\phi'(k, l)$ in the y direction, i.e. orthogonal to the direction of line scan.

The power spectral-density of the electrical fluctuations due to granularity is the Fourier transform of the temporal autocorrelation function of the electrical signal. For example, the temporal autocorrelation function $\phi''(\tau)$ shown in Fig. 19(b) can be written

$$\phi''(\tau) \equiv \phi_h'(\tau) + \phi_i'(\tau \pm T) + \phi_j'(\tau \pm 2T) + \phi_m'(\tau \pm 3T) \quad (12)$$

where the subscripts denote the functions given by the corresponding plane sections of the spatial autocorrelation function $\phi'(k, l)$ indicated in Fig. 19(a). The Fourier transform $N''(f)$ of $\phi''(\tau)$ can be written

$$\begin{aligned} N''(f) = & \left[\phi_h'(\tau) \right]^* + (2 \cos 2\pi f T) \left[\phi_i'(\tau) \right]^* \\ & + (2 \cos 4\pi f T) \left[\phi_j'(\tau) \right]^* \\ & + (2 \cos 6\pi f T) \left[\phi_m'(\tau) \right]^* \end{aligned} \quad (13)$$

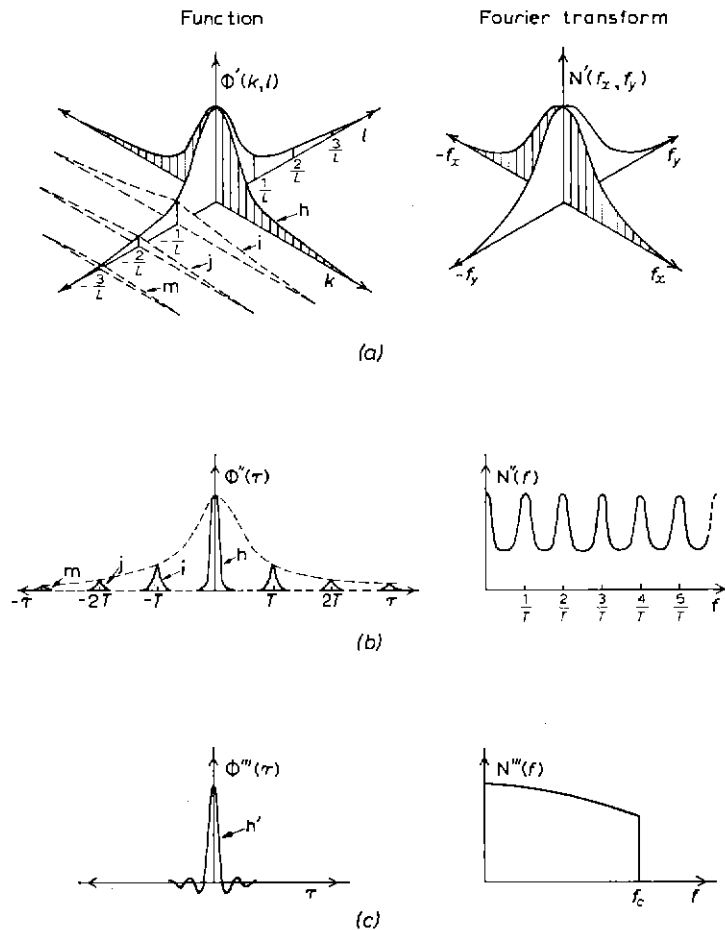


Fig. 19 — Analysis functions and their Fourier transforms

where the asterisk denotes 'Fourier transform of' and the frequency variable, f , is now temporal. Thus the power spectral density is seen to be, in general, quasi-periodic with maxima occurring at integral multiples of the line-scan frequency $1/T$, as illustrated in the right hand diagram of Fig. 19(b). The sharpness of the maxima will depend on the number of harmonic terms in equation (13), and the locus of the peaks is given by

$$N''(f) = \left[\phi_h'(\tau) \right]^* + 2 \left[\phi_i'(\tau) \right]^* + 2 \left[\phi_j'(\tau) \right]^* - 2 \left[\phi_m'(\tau) \right]^* \quad (14)$$

Now, we see from Fig. 19(a) that an approximation to function $N'(f_x, 0)$, i.e. the principal section of $N'(f_x, f_y)$ in the x direction, is

$$N'(f_x, 0) \simeq C \left\{ \left[\phi_h'(k, 0) \right]^* + 2 \left[\phi_i'(k, 1/L) \right]^* + 2 \left[\phi_j'(k, 2/L) \right]^* + 2 \left[\phi_m'(k, 3/L) \right]^* \right\} \quad (15)$$

if we suppose the grain autocorrelation function $\phi'(k, l)$ to

be represented by its plane sections denoted by $h, \pm i, \pm j, \pm m$, and C to be a suitable constant. Hence, comparing equations (14) and (15), we can infer that when the scanning line density is high, leading to pronounced peaks in the fine structure of the electrical power spectrum, the form of the locus of the peaks is given approximately by $N'(f_x, 0)$.

The effects of video equalization and bandwidth-limiting on the autocorrelation function are to modify the shape of the pulses forming the temporal autocorrelation function. For example, due to some equalization and sharp bandwidth-limiting the central pulse h in Fig. 19(b) will be modified to produce the approximate $(\sin \omega\tau)/\omega\tau$ pulse-shape, h' , shown in Fig. 19(c).

At the receiver, we have to consider the two-dimensional autocorrelation functions of the spatial fluctuations in the displayed luminance due to the film granularity modified, as indicated above, by the transmission process. If we first assume that the display-tube scanning spot is infinitely fine, the autocorrelation function of the displayed granularity, $A(k, l)$, will be similar to that shown at (f) in Fig. 20. This function consists of a set of vertical plane sections, lying in the line-scan direction, spaced in the orthogonal direction at equal intervals of $1/L$, where L is now the line-

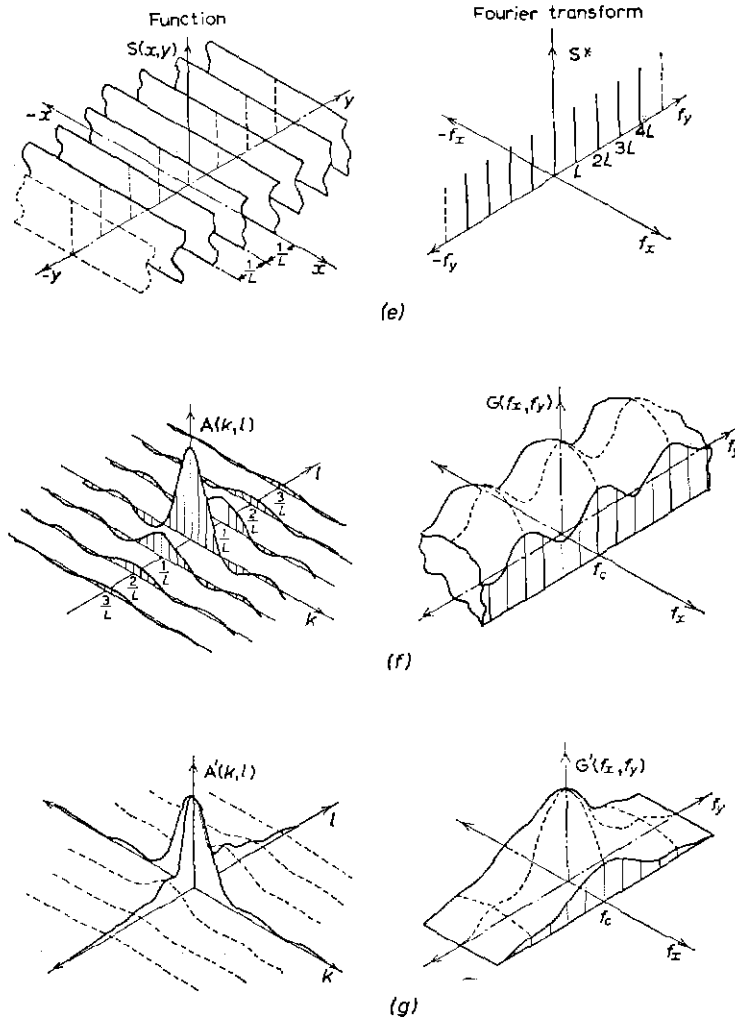


Fig. 20 — Synthesis functions and their Fourier transforms

density of the display scan. The autocorrelation function is zero between the sections and the shapes of the sections are similar to that shown in Fig. 19(c).

Alternatively, the function $A(k,l)$ can be generated as follows: Multiply the original grain Wiener spectrum, $N(f_x, f_y)$, by the square of the modulus of the overall frequency response function of the television system (excluding the display-tube scanning spot). Deduce the Fourier transform of this product and then multiply the transform by the function $S(x,y)$ shown at (e) in Fig. 20. Thus $A(k,l)$ is obtained.

The 'bean-slicer' function $S(x,y)$ is the functional representation of the scanning process; and consists of an infinite number of parallel planes, equally spaced at intervals of $1/L$, of unit height and unbounded in the direction of line scan. Thus any right section of the function, other than the x direction, consists of an infinite set of equally-spaced unit impulses, i.e. a Dirac 'comb', as it is sometimes termed. The Fourier transform of $S(x,y)$ is also a Dirac 'comb', lying in the y direction, with 'teeth' located at

$f_y = 0 \pm L, \pm 2L, \pm 3L, \pm \dots \infty$, as illustrated by the function S^* in Fig. 20(e).

Now, since $A(k,l)$ is the product of $S(x,y)$ with the system-modified grain autocorrelation function, the transform of $A(k,l)$ will be the convolution of the system-weighted grain Wiener spectrum with the function S^* . The result is shown by the solid function $G(f_x, f_y)$ in Fig. 20(f); right sections of this function parallel to the y direction are periodic and unbounded; while in the x direction, right sections are aperiodic and bounded at the spatial frequencies $\pm f_c$.

The function $G(f_x, f_y)$ can be regarded as the Wiener spectrum of the displayed granularity for an infinitely fine display-tube scanning spot. The final operation must, therefore, be the spectral weighting due to the spatial finiteness of the tube spot. Hence one might expect to obtain, finally, the Wiener spectrum $G'(f_x, f_y)$ and the corresponding autocorrelation function $A'(k,l)$ shown at (g) in Fig. 20. It will be noted that $A'(k,l)$ is now a solid function.